

Spin-orbit torques and tunable Dzyaloshinskii-Moriya interaction in Co/Cu/Co trilayers

Frank Freimuth,* Stefan Blügel, and Yuriy Mokrousov
*Peter Grünberg Institut and Institute for Advanced Simulation,
 Forschungszentrum Jülich and JARA, 52425 Jülich, Germany*
 (Dated: May 16, 2018)

We study the spin-orbit torques (SOTs) in Co/Cu/Co magnetic trilayers based on first-principles density-functional theory calculations in the case where the applied electric field lies in-plane, i.e., parallel to the interfaces. We assume that the bottom Co layer has a fixed in-plane magnetization, while the top Co layer can be switched. We find that the SOT on the top ferromagnet can be controlled by the bottom ferromagnet because of the nonlocal character of the SOT in this system. As a consequence the SOT is anisotropic, i.e., its magnitude varies with the direction of the applied electric field. We show that the Dzyaloshinskii-Moriya interaction (DMI) in the top layer is anisotropic as well, i.e., the spin-spiral wavelength of spin-spirals in the top layer depends on their in-plane propagation direction. This effect suggests that DMI can be tuned easily in magnetic trilayers via the magnetization direction of the bottom layer. In order to understand the influence of the bottom ferromagnet on the SOTs and the DMI of the top ferromagnet we study these effects in Co/Cu magnetic bilayers for comparison. We find the SOTs and the DMI to be surprisingly large despite the small spin-orbit interaction of Cu.

I. INTRODUCTION

In noncentrosymmetric ferromagnets the application of an electric current generates torques on the magnetization that result from the spin-orbit interaction (SOI) and that can be used to switch the magnet (see Ref. [1] for a recent review). In magnetic bilayers such as Co/Pt, CoFeB/Ta and CoFeB/W with structural inversion asymmetry spin currents mediate an important contribution to these so-called spin-orbit torques (SOTs) [2–5]. At first, these spin currents were generated by the spin Hall effect (SHE) of nonmagnetic heavy metals such as Pt, W, Ta and Pd. Later, also the antiferromagnets MnPt, MnPd and MnIr were found to be efficient sources of spin currents due to their large SHE angles [6–8]. Additionally, it has been pointed out that also the anomalous Hall effect (AHE) and the anisotropic magnetoresistance (AMR) of ferromagnets can be used to generate transverse spin currents, because the transverse charge currents from the AHE and from the planar Hall effect are spin-polarized [9]. Another contribution to the SOT in magnetic bilayers stems from the interfacial SOI [10–12].

Recently, switching of the magnetization by SOT has been demonstrated in CoFeB/Ti/CoFeB magnetic trilayers [13]. In the trilayer two CoFeB ferromagnets (one at the top and one at the bottom) are separated by a Ti normal metal spacer (see Fig. 1 for illustration of a Co/Cu/Co trilayer). The magnetization of the bottom ferromagnet (FM) is fixed to the in-plane x direction. In order to switch the top FM an electric current is applied parallel to the magnetization of the bottom FM. Experiments show that the spin current that switches the top magnet is generated at the interface between the bottom magnet and the normal metal (NM) spacer and that

the spin polarization of the spin current has components along both the y and the z direction [13, 14].

Such interface-generated spin currents can be explained in terms of spin-orbit filtering and spin-orbit precession [15–17] and provide a third mechanism for SOTs, which adds to the two mechanisms found in magnetic bilayers, i.e., the contribution from the SHE and the contribution from the interfacial SOI at the interface between the top magnet and the normal metal. Since the spin polarization of the spin current has a component along the z direction, the magnetization can be switched deterministically by the applied electric current without the need for additional external magnetic fields. While it has been observed in *ab-initio* calculations [18, 19] on magnetic bilayers that SHE angles are position-dependent and can be strongly enhanced close to interfaces, the interface-generated spin currents from the bottom FM interface exhibit a distinct spin polarization, which can be controlled by the bottom FM magnetization direction.

Magnetic bilayer structures such as Co/Pt are often rotationally symmetric around the interface normal direction when the magnetization points out-of-plane [5]. In such cases the magnitude of the SOT does not depend on the in-plane direction of the applied electric current. However, when the bottom FM magnetization in a trilayer lies in-plane and the top FM magnetization points out-of-plane, this symmetry is broken, i.e., the SOTs exerted on the top FM are expected to depend on the direction of the applied electric current. Since it has been found that SOTs and the Dzyaloshinskii-Moriya interaction (DMI) are correlated in various ways [20–22], one may expect that also the DMI is anisotropic in this case such that the wavelength of spin spirals that are stabilized by DMI depends on the in-plane direction of the spin-spiral wave vector. Equivalently, when a spin spiral

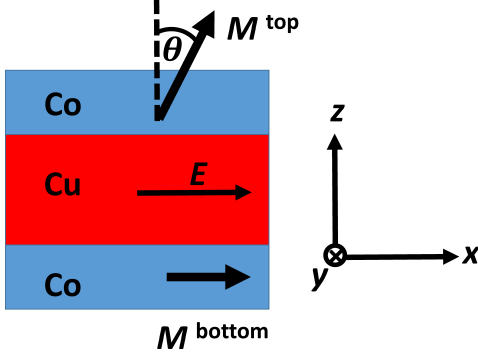


FIG. 1: Illustration of a Co/Cu/Co trilayer structure. The magnetization of the top layer, \mathbf{M}^{top} , can be switched, while the magnetization of the bottom layer, $\mathbf{M}^{\text{bottom}}$, is fixed to point into the x direction. The two Co-ferromagnets are separated by a Cu normal metal spacer. The applied electric field \mathbf{E} points in the in-plane direction, e.g. in x direction as shown in the figure. The interface normal direction, i.e., the out-of-plane direction, points in z direction.

in the top FM is oriented in a fixed direction, the spin-spiral wavelength can be tuned by the magnetization direction in the bottom FM. Compared to other methods of tuning the DMI, which require to generate a strong non-equilibrium situation by applying femtosecond laser pulses [23, 24], the option to tune DMI via the magnetization direction of the bottom FM is attractive by its simplicity.

In this work we investigate SOTs and DMI in Co/Cu/Co trilayers and in Co/Cu bilayers. These systems are ideal to investigate SOTs that arise from interface-generated spin currents, because the SHE angle of bulk Cu is negligibly small and therefore the possibility that there might be contributions to the SOT originating from the SHE of bulk Cu can be ruled out. So far, current-induced torques in Co/Cu/Co spin-valves have been investigated experimentally [25] and theoretically [26, 27] only in the current perpendicular to the plane (CPP) geometry. Only in Co/Cu bilayers the field-like component of the SOT has been investigated already theoretically for the case of electric current applied parallel to the interfaces [28].

This paper is organized as follows. In Sec. II we discuss the symmetry of the SOTs in Co/Cu/Co trilayers. In Sec. III we explain the formalism that we use in order to calculate SOTs and DMI in these systems. In Sec. IV we discuss the *ab-initio* results for the SOTs in Co/Cu/Co trilayers and in Co/Cu bilayers. In Sec. V we present our result on the DMI in these systems. This paper ends with a summary in Sec. VI.

II. SYMMETRY PROPERTIES

We consider a Co/Cu/Co trilayer as illustrated in Fig. 1. We assume that the Co and Cu layers are stacked along their (001) directions. In this case, the crystal lattice of the trilayer has $c4$ rotational symmetry around the z axis and the planes xz and yz are mirror planes of the crystal lattice. We assume that the magnetization of the bottom FM, $\hat{\mathbf{M}}^{\text{bottom}}$, points into the x direction, while the magnetization direction of the top FM is given by $\hat{\mathbf{M}}^{\text{top}} = (\sin \theta \cos \phi, \sin \theta \sin \phi, \cos \theta)^T$. In order to describe the torque \mathbf{T}^{top} on the top FM we define the torque tensor \mathbf{t}^{top} such that

$$\mathbf{T}^{\text{top}} = \mathbf{t}^{\text{top}} \mathbf{E}. \quad (1)$$

We first consider the case with $\theta = 0$ and $\phi = 0$ when the electric field is applied in x direction. Since the torque is perpendicular to the magnetization we only need to consider the two components T_x^{top} and T_y^{top} . The xz mirror plane flips $\hat{\mathbf{M}}^{\text{top}}$, $\hat{\mathbf{M}}^{\text{bottom}}$, and T_x^{top} (because they are axial vectors), but it leaves E_x (polar vector) and T_y^{top} unchanged. The $c2$ rotation around the z axis flips all in-plane vector components. Thus, combination of the xz mirror plane and the $c2$ rotation around the z axis leaves T_x^{top} and $\hat{\mathbf{M}}^{\text{bottom}}$ unchanged, but flips E_x , T_y^{top} , and $\hat{\mathbf{M}}^{\text{top}}$. Consequently, T_x^{top} is odd in $\hat{\mathbf{M}}^{\text{top}}$, i.e., T_x^{top} changes sign when $\hat{\mathbf{M}}^{\text{top}}$ is flipped. Additionally, T_y^{top} is even in the magnetization $\hat{\mathbf{M}}^{\text{top}}$, i.e., it does not change sign when $\hat{\mathbf{M}}^{\text{top}}$ is flipped. When the electric field is applied in y direction, the combination of the xz mirror plane and of the $c2$ rotation around the z axis preserves E_y . Therefore, T_x^{top} is even in $\hat{\mathbf{M}}^{\text{top}}$, and T_y^{top} is odd in $\hat{\mathbf{M}}^{\text{top}}$ when the electric field is applied in y direction. Since the $c2$ rotation around the z axis flips the applied electric field, $\hat{\mathbf{M}}^{\text{bottom}}$, T_x^{top} , and T_y^{top} , it follows that both T_x^{top} and T_y^{top} are even in $\hat{\mathbf{M}}^{\text{bottom}}$. These properties are summarized in the first row of Table I and in the first row of Table II.

Next, we consider the case with $\theta = 90^\circ$ and $\phi = 0^\circ$. The magnetizations of both the top FM and the bottom FM point in x direction in this case. Since the torque is perpendicular to the magnetization we only consider T_y^{top} and T_z^{top} . We first assume that the electric field is applied in x direction. The xz mirror plane preserves E_x and T_y^{top} , but it flips T_z^{top} , $\hat{\mathbf{M}}^{\text{top}}$ and $\hat{\mathbf{M}}^{\text{bottom}}$. Consequently, T_y^{top} does not change when both $\hat{\mathbf{M}}^{\text{top}}$ and $\hat{\mathbf{M}}^{\text{bottom}}$ are flipped, while T_z^{top} changes sign in this case. When the electric field is applied in y direction, the yz mirror plane preserves E_y , $\hat{\mathbf{M}}^{\text{top}}$, and $\hat{\mathbf{M}}^{\text{bottom}}$, but it flips both T_y^{top} and T_z^{top} . Thus, symmetry requires $t_{yy}^{\text{top}} = 0$ and $t_{zy}^{\text{top}} = 0$. These properties are summarized in the second row of Table II.

TABLE I: Symmetry properties of the torkance tensor t_{ij}^{top} for various directions of the magnetization $\hat{\mathbf{M}}^{\text{top}} = (\sin \theta \cos \phi, \sin \theta \sin \phi, \cos \theta)^T$. + means that the torkance is even in $\hat{\mathbf{M}}^{\text{top}}$ (i.e., it does not change sign when $\hat{\mathbf{M}}^{\text{top}}$ is flipped while $\hat{\mathbf{M}}^{\text{bottom}}$ is not flipped) and - means that the torkance is odd in $\hat{\mathbf{M}}^{\text{top}}$ (i.e., it changes sign when $\hat{\mathbf{M}}^{\text{top}}$ is flipped while $\hat{\mathbf{M}}^{\text{bottom}}$ is not flipped).

	t_{xx}^{top}	t_{xy}^{top}	t_{yx}^{top}	t_{yy}^{top}	t_{zx}^{top}	t_{zy}^{top}
$\theta = 0, \phi = 0$	-	+	+	-	0	0
$\theta = 90^\circ, \phi = 90^\circ$	-	+	0	0	+	-

TABLE II: Symmetry properties of the torkance tensor t_{ij}^{top} for various directions of the magnetization $\hat{\mathbf{M}}^{\text{top}} = (\sin \theta \cos \phi, \sin \theta \sin \phi, \cos \theta)^T$. + means that the torkance does not change sign when both $\hat{\mathbf{M}}^{\text{top}}$ and $\hat{\mathbf{M}}^{\text{bottom}}$ are flipped. - means that the torkance changes sign when both $\hat{\mathbf{M}}^{\text{top}}$ and $\hat{\mathbf{M}}^{\text{bottom}}$ are flipped.

	t_{xx}^{top}	t_{xy}^{top}	t_{yx}^{top}	t_{yy}^{top}	t_{zx}^{top}	t_{zy}^{top}
$\theta = 0, \phi = 0$	-	+	+	-	0	0
$\theta = 90^\circ, \phi = 0$	0	0	+	0	-	0
$\theta = 90^\circ, \phi = 90^\circ$	+	+	0	0	-	-

Finally, we consider the case where $\hat{\mathbf{M}}^{\text{top}}$ points in y direction, i.e., $\theta = 90^\circ$ and $\phi = 90^\circ$. Since the torque is perpendicular to the magnetization we only need to consider T_x^{top} and T_z^{top} . First, we assume that the electric field is applied in x direction. The xz mirror plane flips T_x^{top} , T_z^{top} and $\hat{\mathbf{M}}^{\text{bottom}}$, but it preserves E_x and $\hat{\mathbf{M}}^{\text{top}}$. Thus, the combination of the c2 rotation around the z axis with the xz mirror plane preserves T_x^{top} and $\hat{\mathbf{M}}^{\text{bottom}}$ but flips E_x , $\hat{\mathbf{M}}^{\text{top}}$ and T_z^{top} . Consequently, T_z^{top} is even in $\hat{\mathbf{M}}^{\text{top}}$ and T_x^{top} is odd in $\hat{\mathbf{M}}^{\text{top}}$. When the electric field points in y direction, the combination of the c2 rotation around the z axis with the xz mirror plane preserves E_y . In this case T_z^{top} is odd in $\hat{\mathbf{M}}^{\text{top}}$ and T_x^{top} is even in $\hat{\mathbf{M}}^{\text{top}}$. A c2 rotation around the z axis flips $\hat{\mathbf{M}}^{\text{top}}$, $\hat{\mathbf{M}}^{\text{bottom}}$, \mathbf{E} , and T_x^{top} but preserves T_z^{top} . Consequently, T_x^{top} does not change sign when both $\hat{\mathbf{M}}^{\text{top}}$ and $\hat{\mathbf{M}}^{\text{bottom}}$ are flipped, while T_z^{top} changes sign when both $\hat{\mathbf{M}}^{\text{top}}$ and $\hat{\mathbf{M}}^{\text{bottom}}$ are flipped. These properties are summarized in the second row of Table I and in the third row of Table II.

The case $\theta = 90^\circ$ and $\phi = 90^\circ$ is of special interest, because it is well-known for magnetic bilayers that $t_{zx} = 0$ and $t_{xx} = 0$ when $\theta = 90^\circ$ and $\phi = 90^\circ$ [5]. Indeed, from Table I and Table II it is clear that t_{zx}^{top} and t_{xx}^{top} cannot exist without the bottom magnetic layer: For $\theta = 90^\circ$ and $\phi = 90^\circ$ t_{zx}^{top} is even in the magnetization of the top layer (see Table I), but odd in the total magnetization (see Table II). Similarly, t_{xx}^{top} is odd in the magnetization of the top layer (see Table I), but even in the total magnetization (see Table II). Clearly, these conditions cannot be satisfied when the bottom magnetic layer is missing.

Since $t_{zx}^{\text{top}} = t_{xx}^{\text{top}} = 0$ in bilayers, the underlying mechanism in trilayers has to involve the bottom FM, i.e., it has to be a nonlocal mechanism. Since nonlocal transfer of angular momentum is mediated by spin currents, we attribute the nonzero t_{zx}^{top} in trilayers to a spin current with spin-polarization along z direction flowing from the bottom FM to the top FM. Such a spin current can be generated at the bottom FM interface through spin-orbit precession [13, 15, 17]. t_{zx}^{top} is odd in the magnetization of the bottom magnet, consistent with the mechanism of spin-orbit precession. As the z -polarized spin current interacts with the top FM it precesses around the top FM magnetization. This leads to an additional torque component in the direction of $\hat{\mathbf{M}}^{\text{top}} \times \hat{\mathbf{e}}_z$, which is odd in $\hat{\mathbf{M}}^{\text{top}}$. For $\hat{\mathbf{M}}^{\text{top}} = \hat{\mathbf{e}}_y$ this torque points into the x direction, which explains the component t_{xx}^{top} . Therefore, both t_{xx}^{top} and t_{zx}^{top} arise from the z -polarized spin current. Since t_{xx}^{top} is odd in the top FM magnetization, it cannot be explained by a spin current with spin-polarization along x that interacts with the top FM through spin transfer, because the resulting torque would be even in $\hat{\mathbf{M}}^{\text{top}}$. The z -polarized spin current in trilayers is of particular interest, because it allows field-free switching and provides an antidamping-torque for the perpendicular top FM [13, 14]. Calculating the SOT at $\theta = \phi = 90^\circ$ is an easy way to investigate this z -polarized spin current. In comparison, the SOT at $\phi = 0^\circ$ and $0 < \theta < 90^\circ$ contains also contributions from the interfacial SOI at the top FM interface and therefore it does not give direct access to the z -polarized spin current.

III. FORMALISM

A. Spin-orbit torque

We define the torkance $t_{ij\alpha}$ of atom α by the equation

$$T_{i\alpha} = \sum_j t_{ij\alpha} E_j, \quad (2)$$

where E_j is the j -th component of the applied electric field and $T_{i\alpha}$ is the i -th component of the torque exerted on the magnetic moment of atom α . In the Co/Cu/Co trilayers considered in this work we will be particularly interested in the sum of $t_{ij\alpha}$ over all atoms in the top FM,

$$t_{ij}^{\text{top}} = \sum_{\alpha \in \text{top}} t_{ij\alpha}, \quad (3)$$

where $\alpha \in \text{top}$ denotes the atoms in the top FM. Since the bottom and top FM are separated by a Cu spacer, the top FM can switch while the bottom FM can be kept fixed. For the magnetization dynamics of the top FM the sum as defined in Eq. (3) is the relevant torkance. In magnetic bilayers with only one ferromagnetic layer,

such as a Co/Cu magnetic bilayer, the relevant torkance is obtained by summing over all atoms, i.e.,

$$t_{ij} = \sum_{\alpha} t_{ij\alpha}. \quad (4)$$

The torkance is given by the sum of three terms, i.e., $t_{ij\alpha} = t_{ij\alpha}^{I(a)} + t_{ij\alpha}^{I(b)} + t_{ij\alpha}^{\Pi}$, where [4, 18]

$$\begin{aligned} t_{ij\alpha}^{I(a)} &= \frac{eA}{h} \int \frac{d^2k}{(2\pi)^2} \text{Tr} \langle \mathcal{T}_{i\alpha} G_{\mathbf{k}}^R(\mathcal{E}_F) v_j G_{\mathbf{k}}^A(\mathcal{E}_F) \rangle \\ t_{ij\alpha}^{I(b)} &= -\frac{eA}{h} \int \frac{d^2k}{(2\pi)^2} \text{Re Tr} \langle \mathcal{T}_{i\alpha} G_{\mathbf{k}}^R(\mathcal{E}_F) v_j G_{\mathbf{k}}^R(\mathcal{E}_F) \rangle \\ t_{ij\alpha}^{\Pi} &= \frac{eA}{h} \int_{-\infty}^{\mathcal{E}_F} d\mathcal{E} \int \frac{d^2k}{(2\pi)^2} \text{Re Tr} \left\langle \mathcal{T}_{i\alpha} G_{\mathbf{k}}^R(\mathcal{E}) v_j \frac{dG_{\mathbf{k}}^R(\mathcal{E})}{d\mathcal{E}} \right. \\ &\quad \left. - \mathcal{T}_{i\alpha} \frac{dG_{\mathbf{k}}^R(\mathcal{E})}{d\mathcal{E}} v_j G_{\mathbf{k}}^R(\mathcal{E}) \right\rangle. \end{aligned} \quad (5)$$

Here, A is the area of the in-plane unit cell, such that $T_{i\alpha}$ in Eq. (2) is the i -th component of the torque exerted on the magnetic moments of atom type α in one unit cell. $e > 0$ is the elementary positive charge, \mathbf{k} denotes a k -point in the two-dimensional Brillouin zone of the bilayers and trilayers, $G_{\mathbf{k}}^R(\mathcal{E})$ is the retarded Green's function, $G_{\mathbf{k}}^A(\mathcal{E})$ is the advanced Green's function, \mathcal{E}_F is the Fermi energy, v_j is the j -th component of the velocity operator, and $\mathcal{T}_{i\alpha}$ is the i -th component of the torque operator \mathcal{T}_{α} of atom α with matrix elements

$$\langle \psi_{\mathbf{k}n} | \mathcal{T}_{\alpha} | \psi_{\mathbf{k}m} \rangle = -\mu_B \int_{\text{MT}_{\alpha}} d^3r \psi_{\mathbf{k}n}^{\dagger}(\mathbf{r}) \boldsymbol{\sigma} \times \boldsymbol{\Omega}^{\text{xc}}(\mathbf{r}) \psi_{\mathbf{k}m}(\mathbf{r}), \quad (6)$$

where μ_B is the Bohr magneton, $\boldsymbol{\sigma}$ is the vector of Pauli spin matrices, $\boldsymbol{\Omega}^{\text{xc}}(\mathbf{r})$ is the exchange field, which is obtained from the difference between the effective potentials of minority and majority electrons as $\boldsymbol{\Omega}^{\text{xc}}(\mathbf{r}) = \frac{1}{2\mu_B} [V_{\text{minority}}^{\text{eff}}(\mathbf{r}) - V_{\text{majority}}^{\text{eff}}(\mathbf{r})] \hat{\mathbf{M}}(\mathbf{r})$, and $\hat{\mathbf{M}}(\mathbf{r})$ is the magnetization direction. The volume integration in Eq. (6) is restricted to the MT-sphere of atom α .

The torkances depend on the magnetization direction $\hat{\mathbf{M}}$. We define the even torkance $t_{ij\alpha}^e(\hat{\mathbf{M}}) = [t_{ij\alpha}(\hat{\mathbf{M}}) + t_{ij\alpha}(-\hat{\mathbf{M}})]/2$ and the odd torkance $t_{ij\alpha}^o(\hat{\mathbf{M}}) = [t_{ij\alpha}(\hat{\mathbf{M}}) - t_{ij\alpha}(-\hat{\mathbf{M}})]/2$. Inversion of magnetization, i.e., $\hat{\mathbf{M}} \rightarrow -\hat{\mathbf{M}}$, does not modify the even torkance, but it flips the sign of the odd torkance. The torkance is the sum of its even and odd parts, i.e., $t_{ij\alpha}(\hat{\mathbf{M}}) = t_{ij\alpha}^e(\hat{\mathbf{M}}) + t_{ij\alpha}^o(\hat{\mathbf{M}})$. $t_{ij\alpha}^{\Pi}$ in Eq. (5) contributes only to $t_{ij\alpha}^e$ and $t_{ij\alpha}^{I(b)}$ contributes only to $t_{ij\alpha}^o$, while $t_{ij\alpha}^{I(a)}$ contributes to both $t_{ij\alpha}^e$ and $t_{ij\alpha}^o$. Since the magnetizations in the top and bottom FMs may point into different directions in trilayers (see Fig. 1), it is important to point out that $t_{ij\alpha}^o(\hat{\mathbf{M}})$ changes sign when both $\hat{\mathbf{M}}^{\text{top}}$ and $\hat{\mathbf{M}}^{\text{bottom}}$ are flipped, while $t_{ij\alpha}^e(\hat{\mathbf{M}})$ does not change sign when

both $\hat{\mathbf{M}}^{\text{top}}$ and $\hat{\mathbf{M}}^{\text{bottom}}$ are flipped, because the odd character of $t_{ij\alpha}^o(\hat{\mathbf{M}})$ and the even character of $t_{ij\alpha}^e(\hat{\mathbf{M}})$ result from their transformation properties under time reversal [4]. Therefore, the even torkance in Co/Cu/Co trilayers corresponds to the plus entries in Table II and the odd torkance corresponds to the minus entries in Table II. As discussed in Table I one can also consider how the torkance changes when only $\hat{\mathbf{M}}^{\text{top}}$ is flipped while $\hat{\mathbf{M}}^{\text{bottom}}$ is kept fixed and in some cases the torkance for $-\hat{\mathbf{M}}^{\text{top}}$ and $+\hat{\mathbf{M}}^{\text{bottom}}$ is simply equal or opposite to the torkance for $+\hat{\mathbf{M}}^{\text{top}}$ and $+\hat{\mathbf{M}}^{\text{bottom}}$. Thus, one can also define even and odd torques with respect to $\hat{\mathbf{M}}^{\text{top}}$ when $\hat{\mathbf{M}}^{\text{bottom}}$ is kept fixed. The fact that the third row in Table II differs from the second row in Table I shows that flipping the bottom magnetization $\hat{\mathbf{M}}^{\text{bottom}}$ may impact the torque on the top magnet. Therefore, in the following we mean by even torque always that the torque does not change when both $\hat{\mathbf{M}}^{\text{top}}$ and $\hat{\mathbf{M}}^{\text{bottom}}$ are flipped, while by odd torque we mean that the torque changes sign when both $\hat{\mathbf{M}}^{\text{top}}$ and $\hat{\mathbf{M}}^{\text{bottom}}$ are flipped.

B. Dzyaloshinskii-Moriya interaction

DMI is a chiral interaction, which modifies the free energy of noncentrosymmetric magnets proportional to the spatial derivatives of the magnetization. The contribution of DMI to the free energy density at position \mathbf{r} can be written as [22]

$$F^{\text{DMI}}(\mathbf{r}) = \sum_{ij} D_{ij}(\hat{\mathbf{M}}(\mathbf{r})) \hat{\mathbf{e}}_i \cdot \left[\hat{\mathbf{M}}(\mathbf{r}) \times \frac{\partial \hat{\mathbf{M}}(\mathbf{r})}{\partial r_j} \right], \quad (7)$$

where $D_{ij}(\hat{\mathbf{M}})$ are the DMI coefficients and $\hat{\mathbf{e}}_i$ is a unit vector pointing in the i th spatial direction. These DMI coefficients can be decomposed into the contributions associated with the magnetic moments of atom type α , which we denote by $D_{ij\alpha}$, such that

$$D_{ij} = \sum_{\alpha} D_{ij\alpha}. \quad (8)$$

In magnetic trilayers such as Co/Cu/Co we will be particularly interested in summing $D_{ij\alpha}$ over the layers of the top magnet in order to quantify the free energy gained due to the DMI when the magnetization in the top layer forms a cycloidal spin spiral while the magnetization in the bottom layer remains unchanged, i.e., we will be interested in the quantity

$$D_{ij}^{\text{top}} = \sum_{\alpha \in \text{top}} D_{ij\alpha}. \quad (9)$$

We evaluate the DMI coefficients associated with the magnetic moments of atom type α from [22, 29, 30]

$$D_{ij\alpha} = \int \frac{d^2k}{(2\pi)^2} \sum_n f_{\mathbf{k}n} [A_{\mathbf{k}n i j \alpha} - (\mathcal{E}_{\mathbf{k}n} - \mu) B_{\mathbf{k}n i j \alpha}], \quad (10)$$

where

$$A_{knij\alpha} = \hbar \sum_{m \neq n} \text{Im} \left[\frac{\langle \psi_{kn} | \mathcal{T}_{i\alpha} | \psi_{km} \rangle \langle \psi_{km} | v_j | \psi_{kn} \rangle}{\mathcal{E}_{km} - \mathcal{E}_{kn}} \right] \quad (11)$$

and

$$B_{knij\alpha} = -2\hbar \sum_{m \neq n} \text{Im} \left[\frac{\langle \psi_{kn} | \mathcal{T}_{i\alpha} | \psi_{km} \rangle \langle \psi_{km} | v_j | \psi_{kn} \rangle}{(\mathcal{E}_{km} - \mathcal{E}_{kn})^2} \right]. \quad (12)$$

Here, \mathcal{E}_{kn} is the band energy of state $|\psi_{kn}\rangle$. Eq. (10) is valid at zero temperature, which is sufficient for this study. The generalization to finite temperatures has been described elsewhere [22, 29, 30]. Eq. (10), Eq. (11), and Eq. (12) differ from previous works [22, 29, 30] by the introduction of the atomic index α and by the use of the atom-resolved torque operator $\mathcal{T}_{i\alpha}$ defined in Eq. (6). This generalization is necessary in order to study the DMI associated with one magnetic layer, e.g. for the top magnet according to Eq. (9), in a magnetic multilayer structure.

IV. SOT IN Co/Cu/Co TRILAYERS

A. Computational details

We calculate SOTs in magnetic trilayers composed of 3 atomic layers of Co, 9 atomic layers of Cu, and 3 atomic layers of Co (abbreviated as Co(3)/Cu(9)/Co(3) in the following). Additionally we compute trilayers with only 3 or 6 instead of 9 Cu layers, which we abbreviate in the following as Co(3)/Cu(3)/Co(3) or Co(3)/Cu(6)/Co(3), respectively. In order to be able to interpret the results on the trilayers we also calculate a Co/Cu bilayer for comparison, which is composed of 3 layers of Co on 9 layers of Cu (abbreviated as Co(3)/Cu(9)). In order to calculate the SOTs we first perform an electronic structure calculation with the FLEUR [31] code using the generalized gradient approximation [32]. We choose the computational unit cell similar to the one in Ref. [26], where the spin-transfer torque in the current-perpendicular-to-plane-geometry was investigated. However, we do not embed the scattering region between semi-infinite leads as in Ref. [26], but instead we set up the system in the film geometry, i.e., we calculate Vacuum/Co(3)/Cu(n)/Co(3)/Vacuum (n=3,6,9), because we study the SOTs driven by an electric current that is applied parallel to the interfaces. For this purpose we use the film mode of FLEUR, which explicitly takes the vacuum regions into account [33]. We choose the coordinate system such that the z axis is perpendicular to the interfaces, while the x and y axes are parallel to the interfaces (see also Fig. 1). Since the magnetization in the top FM needs to point into a different direction than the magnetization in the bottom FM of

the Co/Cu/Co trilayer, we use the noncollinear mode of FLEUR [34]. The magnetization of the bottom FM points in x direction in our calculations. We specify the magnetization direction of the top FM in terms of angles θ and ϕ , i.e., $\mathbf{m} = (\sin \theta \cos \phi, \sin \theta \sin \phi, \cos \theta)^T$. We include SOI in the calculations. The computational unit cell of the Co(3)/Cu(9)/Co(3) trilayer contains 15 atoms in total. Both Co and Cu are treated as fcc with lattice constant 3.54 Å. Consequently, the distance between adjacent planes is 1.77 Å. The MT-radii of Co and Cu are set to 1.22 Å.

We label the three Co-layers in the top FM as Co-1, Co-2, and Co-3, where Co-1 is adjacent to vacuum and Co-3 faces the Cu-layer. We denote the three Co-layers in the bottom FM by Co-4, Co-5, and Co-6, where Co-4 is adjacent to the Cu-layer and Co-6 faces vacuum. In the Co(3)/Cu(9)/Co(3) trilayer the Cu-layers are labelled Cu-1 through Cu-9, where Cu-1 is adjacent to Co-3 of the top FM.

As explained in Ref. [4] we use Wannier interpolation [35] in order to evaluate Eq. (5) for the SOT and Eq. (10) for the DMI computationally efficiently. For this purpose, we generate 18 maximally localized Wannier functions (MLWFs) per atom using our interface [36] between the FLEUR code and the Wannier90 code [37]. For the generation of MLWFs we used an $8 \times 8 \mathbf{k}$ mesh and as trial orbitals we chose $6 sp^3 d^2$, d_{xy} , d_{yz} , and d_{zx} for spin-up and for spin-down, i.e., 18 trial orbitals per atom. In the case of the Co(3)/Cu(9)/Co(3) trilayer we generated 270 MLWFs, which we disentangled from 378 bands. In the case of the Co(3)/Cu(9) bilayer we generated 216 MLWFs, which we disentangled from 304 bands.

In order to investigate the role of spin-orbit coupling in the normal metal spacer layer we also compute the SOTs in Co(3)/Pt(13)/Co(3) trilayers, where Pt provides strong SOI. The computational details of the Co/Pt/Co trilayer are given in Ref. [4].

B. Even SOT

In Fig. 2 we show the even torkance of the top FM (see Eq. (3)) in the Co(3)/Cu(9)/Co(3) trilayer as a function of the Fermi energy \mathcal{E}_F for a lifetime broadening of $\Gamma = 25 \text{ meV}$ when the magnetization of the top FM points in z direction, i.e., $\theta = \phi = 0$. By plotting the results as a function of \mathcal{E}_F we can roughly anticipate chemical trends: Negative \mathcal{E}_F mimics the system $\text{Fe}_x\text{Co}_{1-x}/\text{Ni}_x\text{Cu}_{1-x}/\text{Fe}_x\text{Co}_{1-x}$ while positive \mathcal{E}_F mimics the system $\text{Ni}_x\text{Co}_{1-x}/\text{Zn}_x\text{Cu}_{1-x}/\text{Ni}_x\text{Co}_{1-x}$. The pure Co(3)/Cu(9)/Co(3) system corresponds to $\mathcal{E}_F = 0$. In agreement with the symmetry analysis in Table II the two nonzero components of the even torkance are $t_{xy}^{\text{top,e}}$ and $t_{yx}^{\text{top,e}}$. Due to the presence of the bottom FM with magnetization in x direction the x and y directions are not equivalent and therefore the torkance components $t_{xy}^{\text{top,e}}$

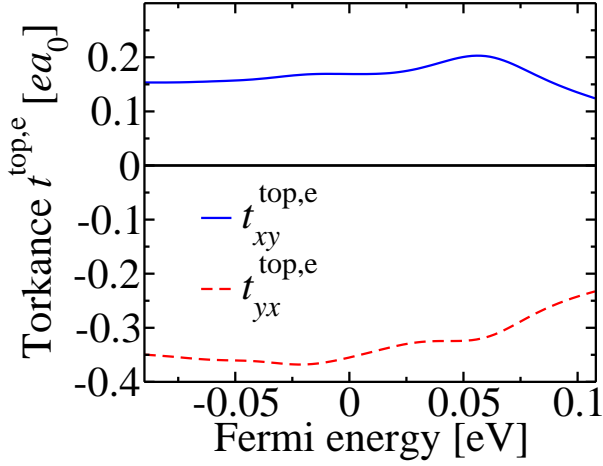


FIG. 2: Even torkance $t_{ij}^{\text{top},e}$ on the top magnetic layer in the Co(3)/Cu(9)/Co(3) magnetic trilayer vs. Fermi energy \mathcal{E}_F when $\theta = \phi = 0$ and $\Gamma = 25\text{meV}$.

and $t_{yx}^{\text{top},e}$ differ substantially (in case of equivalent x and y directions $t_{xy} = -t_{yx}$ would hold). For the range of \mathcal{E}_F shown in the Figure, $t_{xy}^{\text{top},e}$ is much larger than $t_{yx}^{\text{top},e}$. This means that when the electric field is applied in x direction, i.e., parallel to the magnetization of the bottom FM, the SOT is much larger than when the electric field is applied perpendicular to the magnetization of the bottom FM.

For comparison we show in Fig. 3 the total even torkance (see Eq. (4)) of the Co(3)/Cu(9) bilayer as a function of Fermi energy \mathcal{E}_F for a lifetime broadening of $\Gamma = 25\text{meV}$ when the magnetization points in z direction. In this case, the SOT in the Co(3)/Cu(9) bilayer is isotropic, i.e., $t_{xy}^e = -t_{yx}^e$. The component t_{xy}^e in Co(3)/Cu(9) is very similar in size to $t_{xy}^{\text{top},e}$ in Co(3)/Cu(9)/Co(3), but $t_{yx}^{\text{top},e}$ in Co(3)/Cu(9)/Co(3) is much larger than t_{yx}^e in Co(3)/Cu(9). Consequently, the bottom magnet with magnetization along x in the Co(3)/Cu(9)/Co(3) trilayer strongly enhances $t_{yx}^{\text{top},e}$, while its effect on $t_{xy}^{\text{top},e}$ is not so strong.

In Fig. 4 we show the even torkance of the top FM (see Eq. (3)) in the Co(3)/Cu(9)/Co(3) trilayer as a function of the lifetime broadening Γ when the magnetization points in z direction ($\theta = 0$). At small broadening $\Gamma = 1\text{meV}$ the component $t_{yx}^{\text{top},e}$ is larger than $t_{xy}^{\text{top},e}$ by a factor of 1.7 and at large broadening $\Gamma = 100\text{meV}$ the component $t_{yx}^{\text{top},e}$ is larger than $t_{xy}^{\text{top},e}$ by a factor of 1.5. Thus, with increasing Γ the influence of the bottom FM on $t_{ij}^{\text{top},e}$ becomes smaller such that the anisotropy of the SOT reduces. This can be explained by assuming that the effect of the bottom FM on $t_{ij}^{\text{top},e}$ is mediated by spin currents that flow between the bottom FM and the top FM. Such a spin-current mediated effect is not possible when the spin-diffusion length is much smaller

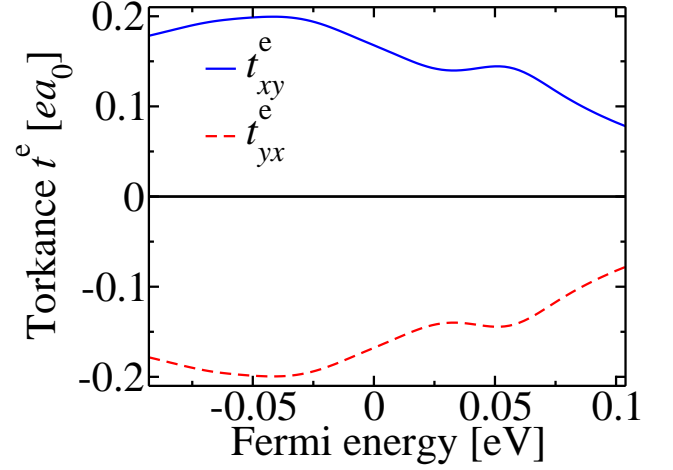


FIG. 3: Even torkance t_{ij}^e in the Co(3)/Cu(9) magnetic bilayer vs. Fermi energy \mathcal{E}_F when $\theta = \phi = 0$ and $\Gamma = 25\text{meV}$.

than the thickness of the Cu spacer layer. Since the spin-diffusion length decreases with increasing disorder, which we model by the broadening Γ , it is expected that an increase of Γ reduces the spin-current-mediated coupling between the bottom and top FMs. The enhancement of $t_{yx}^{\text{top},e}$ in comparison to $t_{xy}^{\text{top},e}$ can be explained by a spin current with spin polarization in y direction, which flows from the bottom FM into the top FM. Such a spin current can be generated through spin-orbit filtering at the bottom FM interface [17]. According to Table I and Table II $t_{yx}^{\text{top},e}$ is even in \hat{M}^{top} and even in \hat{M}^{bottom} , consistent with this mechanism. In order to describe the spin-orbit filtering quantitatively, a model has been proposed that predicts this contribution to be proportional to the relaxation time τ [17]. Since $\tau \propto \hbar/(2\Gamma)$, one expects the contribution from spin-orbit filtering to decrease with increasing Γ . Therefore, there are two reasons why the enhancement of $t_{yx}^{\text{top},e}$ in comparison to $t_{xy}^{\text{top},e}$ decreases with increasing Γ : The spin-current is attenuated stronger on the way from the bottom FM to the top FM and the amount of spin current generated at the bottom FM interface through spin-orbit filtering decreases.

For comparison, we show in Fig. 5 the total even torkance (see Eq. (4)) in the Co(3)/Cu(9) bilayer as a function of lifetime broadening Γ . At large broadening $\Gamma = 100\text{meV}$ $t_{xy}^{\text{top},e}$ in the Co(3)/Cu(9)/Co(3) trilayer is larger than t_{xy}^e in the Co(3)/Cu(9) bilayer by 10% while at small broadening $\Gamma = 1\text{meV}$ $t_{xy}^{\text{top},e}$ in the Co(3)/Cu(9)/Co(3) trilayer is larger than t_{xy}^e in the Co(3)/Cu(9) bilayer by 24%. This trend can be explained again by assuming that the effect of the bottom FM on the top FM is mediated by spin-currents and that this contribution reduces when the disorder increases. Similarly, $t_{yx}^{\text{top},e}$ in the Co(3)/Cu(9)/Co(3) trilayer is larger than t_{yx}^e in the Co(3)/Cu(9) bilayer by 66%

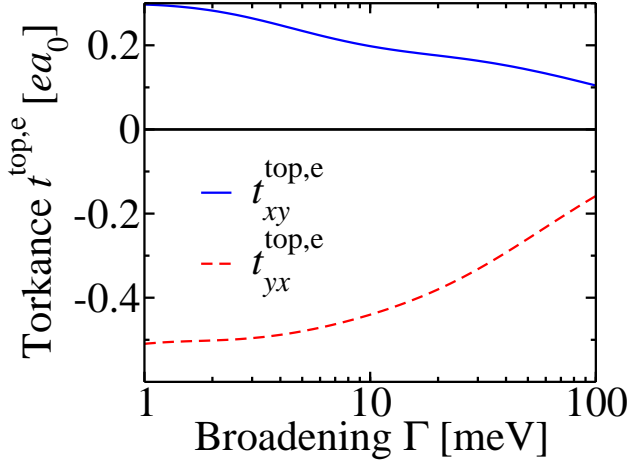


FIG. 4: Even torkance $t_{ij}^{\text{top},e}$ on the top magnetic layer in the Co(3)/Cu(9)/Co(3) magnetic trilayer vs. lifetime broadening Γ when $\theta = \phi = 0$.

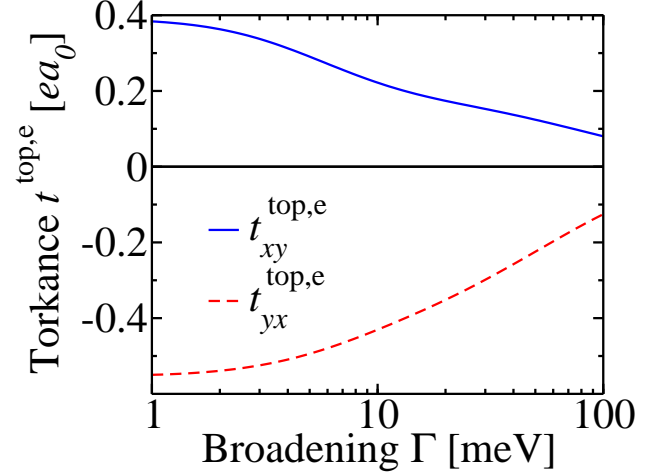


FIG. 6: Even torkance $t_{ij}^{\text{top},e}$ on the top magnetic layer in the Co(3)/Cu(9)/Co(3) magnetic trilayer vs. lifetime broadening Γ when $\theta = \phi = 0$ and when SOI on the Cu atoms is switched off.

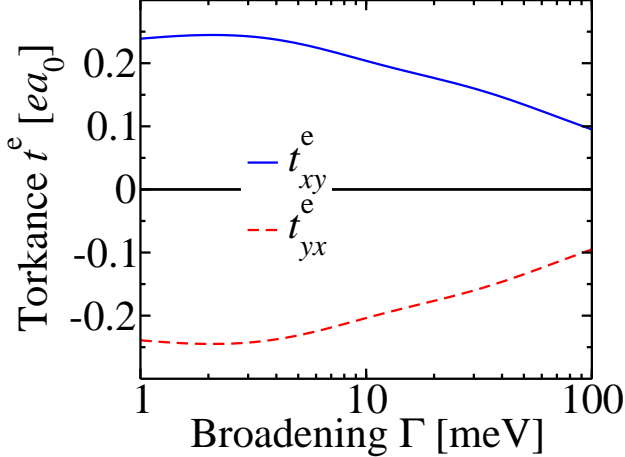


FIG. 5: Even torkance t_{ij}^e in the Co(3)/Cu(9) magnetic bilayer vs. lifetime broadening Γ when $\theta = \phi = 0$.

at large broadening $\Gamma = 100 \text{ meV}$, while at small broadening $\Gamma = 1 \text{ meV}$ $t_{yx}^{\text{top},e}$ in the Co(3)/Cu(9)/Co(3) trilayer is larger than t_{yx}^e in the Co(3)/Cu(9) bilayer by 113%.

Since the SOI in Cu is small, one may expect that it does not contribute to the even torque. In order to verify this by calculations we switch off SOI on all Cu atoms. The resulting even torkance on the top magnetic layer is shown in Fig. 6 as a function of broadening Γ when magnetization points in z direction ($\theta = 0$). In comparison with Fig. 4 the even torkances are quite similar. Therefore, while switching off SOI on Cu obviously has an effect on the torkances it is certainly not the dominant source of $t_{ij}^{\text{top},e}$. This is a major difference to Co/Pt bilayers, where SOI in Pt provides a strong SHE.

In order to investigate the dependence on the thick-

ness of the Cu layer, we show in Fig. 7 the even torkance $t_{ij}^{\text{top},e}$ of the Co(3)/Cu(3)/Co(3) trilayer, in which the spacer consists of only 3 atomic layers of Cu, and in Fig. 8 we show the even torkance $t_{ij}^{\text{top},e}$ of Co(3)/Cu(6)/Co(3), which contains 6 layers of Cu in the spacer layer. At large broadening of $\Gamma = 100 \text{ meV}$ the three systems Co(3)/Cu(3)/Co(3), Co(3)/Cu(6)/Co(3), and Co(3)/Cu(9)/Co(3) exhibit very similar even torkances, but at smaller broadenings the torkances vary differently with Γ . That the torkance becomes independent of the layer thicknesses when Γ is sufficiently large has been found also for Co/Pt bilayers [4]. The component $t_{yx}^{\text{top},e}$ is enhanced in comparison to $t_{xy}^{\text{top},e}$ in both Co(3)/Cu(3)/Co(3) and Co(3)/Cu(6)/Co(3) at small broadening Γ , similar to Co(3)/Cu(9)/Co(3) discussed above.

Next, we discuss how the even SOT depends on the direction of $\hat{\mathbf{M}}^{\text{top}}$. Since the torque is always perpendicular to the magnetization, it is convenient to discuss it using the unit vectors of the spherical coordinate system

$$\hat{\mathbf{e}}_\theta = (\cos \theta \cos \phi, \cos \theta \sin \phi, -\sin \theta)^T \quad (13)$$

and

$$\hat{\mathbf{e}}_\phi = (-\sin \phi, \cos \phi, 0)^T. \quad (14)$$

We define the torkances $t_{\theta i}^{\text{top}}$ and $t_{\phi i}^{\text{top}}$ through

$$\mathbf{T}^{\text{top}} \cdot \hat{\mathbf{e}}_\theta = \sum_i t_{\theta i}^{\text{top}} E_i \quad (15)$$

and

$$\mathbf{T}^{\text{top}} \cdot \hat{\mathbf{e}}_\phi = \sum_i t_{\phi i}^{\text{top}} E_i. \quad (16)$$

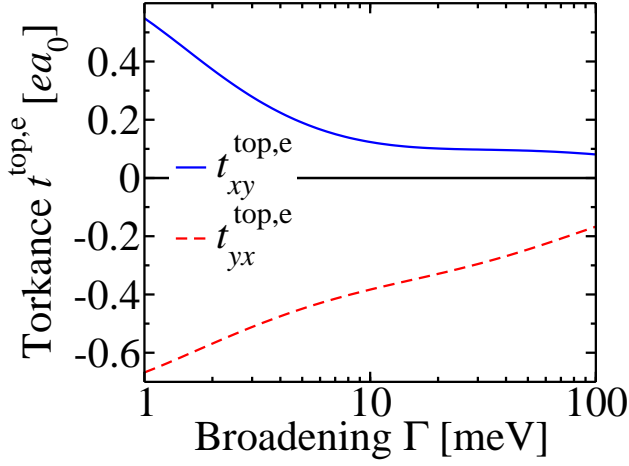


FIG. 7: Even torkance $t_{ij}^{\text{top},e}$ in the Co(3)/Cu(3)/Co(3) magnetic trilayer vs. lifetime broadening Γ when $\theta = \phi = 0$.

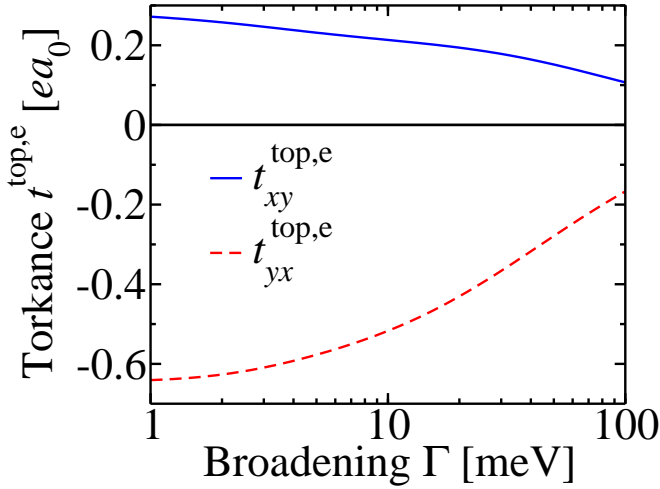


FIG. 8: Even torkance $t_{ij}^{\text{top},e}$ in the Co(3)/Cu(6)/Co(3) magnetic trilayer vs. lifetime broadening Γ when $\theta = \phi = 0$.

In Fig. 9 we show the even torkance in the Co(3)/Cu(9)/Co(3) trilayer as a function of the angle θ when $\phi = 0$ and $\Gamma = 25\text{meV}$. In agreement with the symmetry analysis in Table II the even SOT is zero for $\theta = 90^\circ$ when the electric current is applied in y direction. However, when the electric field is applied in x direction, the even torkance increases strongly from $t_{\phi x}^e = -0.36ea_0$ (at $\theta = 0^\circ$) to $t_{\phi x}^e = -0.88ea_0$ (at $\theta = 90^\circ$). A similarly strong increase of the even torkance with the magnetization angle has been found in experiments on MgO/CoFeB/Ta [5].

In Fig. 10 we show the even torkance as a function of Fermi energy \mathcal{E}_F when $\theta = \phi = 90^\circ$. In agreement with the symmetry analysis in Table II the even SOT points in x direction in this case and it can be generated by an electric field in x direction, but also by an electric

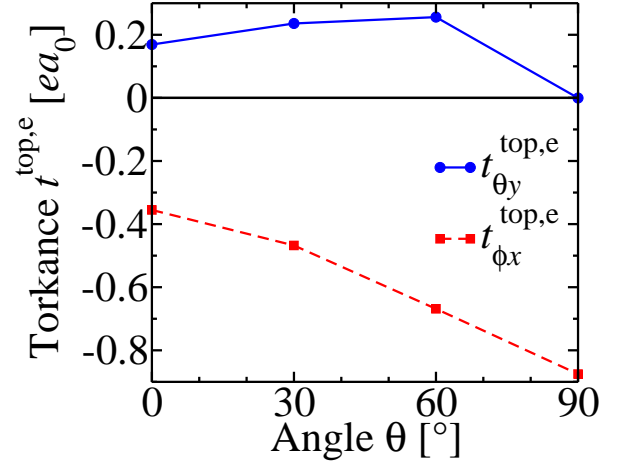


FIG. 9: Even torkance $t_{\theta y}^{\text{top},e}$ (circles) and even torkance $t_{\phi x}^{\text{top},e}$ (squares) in the Co(3)/Cu(9)/Co(3) magnetic trilayer vs. angle θ when $\phi = 0$ and $\Gamma = 25\text{meV}$. Lines serve as guide to the eye.

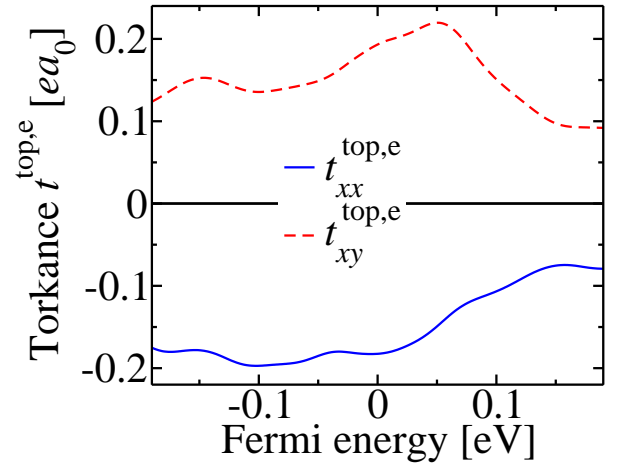


FIG. 10: Even torkance $t_{ij}^{\text{top},e}$ in the Co(3)/Cu(9)/Co(3) magnetic trilayer vs. Fermi energy \mathcal{E}_F when $\theta = \phi = 90^\circ$ and $\Gamma = 25\text{meV}$.

field in y direction. As discussed at the end of section Sec. II, $t_{xx}^{\text{top},e}$ can be explained by a spin current with spin-polarization in z direction, which flows from the bottom magnet into the top magnet, and which precesses around the top FM magnetization, thereby generating a torque in the direction $\hat{M}^{\text{top}} \times \hat{e}_z = \hat{e}_y \times \hat{e}_z = \hat{e}_x$.

In order to compare the SOTs in Co/Cu/Co trilayers, which contain only $3d$ transition metals, to Co/Pt/Co trilayers, in which Pt provides a large SHE, we show in Fig. 11 the even torkance in Co/Pt/Co as a function of broadening Γ when $\theta = \phi = 0$. Similar to the Co/Cu/Co trilayers, $t_{yx}^{\text{top},e}$ is enhanced when compared to $t_{xy}^{\text{top},e}$ at small broadening Γ due to the presence of the bottom

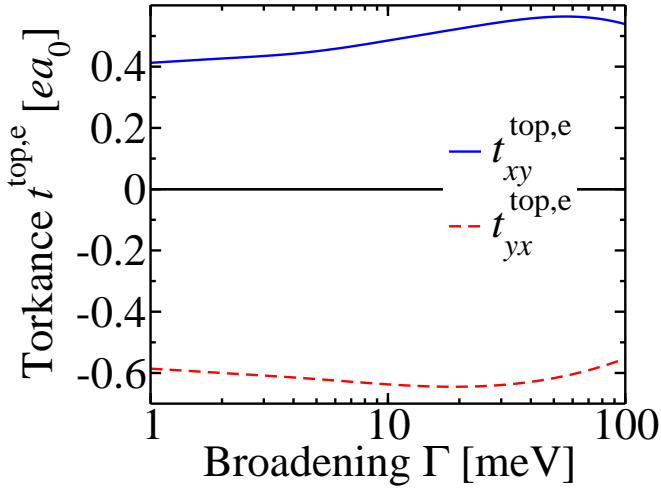


FIG. 11: Even torkance $t_{ij}^{\text{top},e}$ in the Co(3)/Pt(13)/Co(3) magnetic trilayer vs. broadening Γ when $\theta = \phi = 0^\circ$.

magnet. The suppression of the SOT with increasing Γ is considerably smaller in the Co/Pt/Co trilayers than in the Co/Cu/Co trilayers, consistent with our interpretation that the SOT in Co/Cu/Co trilayers arises from different mechanisms. For small broadening Γ the even torkances in Co/Cu/Co and Co/Pt/Co are of the same order of magnitude.

At first glance it is surprising that the even torkances in Co/Cu/Co trilayers are comparable in magnitude to those in Co/Pt bilayers [4, 18] and to those in the Co/Pt/Co trilayers considered here, despite the absence of any 5d or 4d transition metals with strong SOI in the former. However, it is well-known that several SOI-generated effects can be large even in systems that do not contain any 5d or 4d transition metals. For example, the intrinsic AHE of bcc Fe [38] is not much smaller than the one of $L1_0$ FePt [39], despite the presence of a 5d element in the latter. Also in the Heusler compound Co_2MnAl the AHE is large even though it is composed only of 3d transition metals [40]. Similarly, the MAE in Fe/MgO [41] is found to be large, despite the absence of 4d and 5d elements with strong SOI.

According to Eq. (2) the torkance specifies the torque per electric field. However, in order to judge whether the SOT in a given system is sufficiently large to make it attractive for applications it is important to know the torque per electric current. The torque per electric current is obtained from the torkance by multiplication with the electrical resistivity, i.e., $T_y/J_x = t_{yx}\rho_{xx}$ for example. Since the resistivity of bulk Cu is much lower than the one of bulk Pt we estimate that the even torque per current in Co(3)/Cu(9) bilayers and in Co(3)/Cu(9)/Co(3) trilayers is smaller by roughly one order of magnitude when compared to Co/Pt or Co/Pt/Co.

This amplification by the longitudinal resistivity ρ_{xx} is also known from the anomalous Hall effect and from

the spin Hall effect, where materials with large Hall angles are most attractive for applications. The Hall angle is the product of the Hall conductivity and the longitudinal resistivity ρ_{xx} . The antiferromagnets MnIr, MnPt and MnPd have spin Hall angles comparable to the one of Pt despite smaller spin Hall conductivities, because they have larger resistivities than Pt [6]. Also the large spin Hall angles of β -W and β -Ta profit from the high longitudinal resistivity ρ_{xx} of the β -phase [2, 3]. In topological insulators one can even achieve infinitely large spin Hall angles, at least theoretically, and thereby generate large SOTs [42]. Therefore, our finding that the even torkances in Co(3)/Cu(9)/Co(3) and Co(3)/Cu(9) are comparable in size to those in Co/Pt and Co/Pt/Co signifies that one may expect sufficiently large torque per current ratios even when only 3d transition metals are involved, provided that the longitudinal resistivity ρ_{xx} is large enough. While we chose for the spacer layer in this study Cu, which is known to be a good conductor in bulk, it can easily be replaced for example by Ti. Alternatively, one may increase the resistivity of Cu by alloying and thereby increase the torque per current ratio. In this sense Co(3)/Cu(9)/Co(3) and Co(3)/Cu(9) can be considered as models of trilayers and bilayers that are composed of 3d transition metals only. In fact, SOT-switching has recently been demonstrated in FM/Ti/CoFeB trilayers [13], which shows that sufficiently large torque per current ratios can indeed be realized even when only 3d transition metals are used.

C. Odd SOT

In Fig. 12 we show the odd torkance of the top FM (see Eq. (3)) in the Co(3)/Cu(9)/Co(3) trilayer as a function of the Fermi energy \mathcal{E}_F for a lifetime broadening of $\Gamma = 25\text{meV}$ when the magnetization of the top FM points in z direction. In agreement with the symmetry analysis in Table II the nonzero components of the odd torkance are $t_{xx}^{\text{top},o}$ and $t_{yy}^{\text{top},o}$. There is a small difference between $t_{xx}^{\text{top},o}$ and $t_{yy}^{\text{top},o}$, i.e., the odd torkance is slightly anisotropic due to the presence of the bottom magnetic layer with magnetization in x direction, which lowers the symmetry. However, this anisotropy is much smaller than in the case of the even torque discussed above in Fig. 2.

For comparison, we show in Fig. 13 the total odd torkance (see Eq. (4)) in the Co(3)/Cu(9) bilayer as a function of the Fermi energy \mathcal{E}_F for a lifetime broadening of $\Gamma = 25\text{meV}$ when the magnetization points in z direction. In this case, the odd torkance in the Co(3)/Cu(9) bilayer is isotropic, i.e., $t_{xx}^o = t_{yy}^o$. The odd torkance in Co(3)/Cu(9) is very similar to the one in the Co(3)/Cu(9)/Co(3) trilayer. Thus, the influence of the bottom magnetic layer on the odd torkance is much smaller than its influence on the even torkance. This shows that the odd SOT is dominantly local, i.e.,

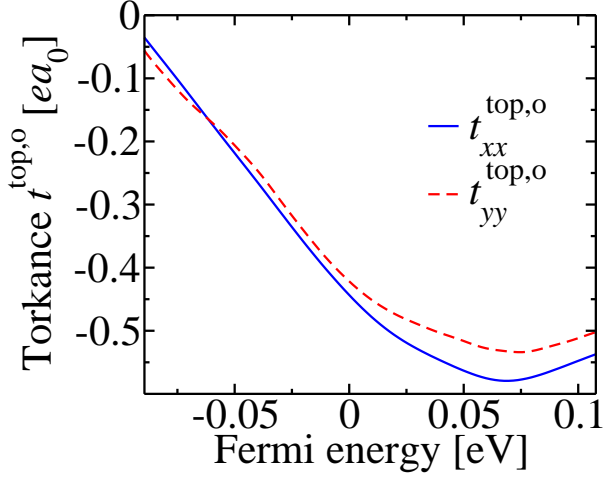


FIG. 12: Odd torkance $t_{ij}^{\text{top},o}$ on the top magnet in the Co(3)/Cu(9)/Co(3) trilayer vs. Fermi energy \mathcal{E}_F when $\theta = \phi = 0$ and $\Gamma = 25\text{meV}$.

it arises from the SOI in the top FM and from the interfacial SOI at the top Co/Cu interface (below we will see that for $\theta = \phi = 90^\circ$ an additional nonlocal contribution to the odd torque can be observed). In contrast, the even SOT in Co(3)/Cu(9)/Co(3) contains an important nonlocal contribution mediated by spin-currents that couple the bottom FM and the top FM. In the pure Co(3)/Cu(9) bilayer ($\mathcal{E}_F = 0$) the odd torkance amounts to $t_{xx}^o = 0.33ea_0$. Interestingly, this value is larger by roughly a factor of four than the odd torkance for a monolayer of Co on Cu(111) obtained from a similar approach with $\Gamma = 25\text{meV}$ (see Fig. 8(b) in Ref. [28]). We attribute this difference to the different interfaces (in the present work the interface normal direction corresponds to the (001) direction of Co and Cu, while in Ref. [28] the interface normal direction corresponds to the (111) direction of Co and Cu) and to the different thicknesses of the Co layer (1 layer of Co in Ref. [28] compared to three layers of Co in the present study).

In Fig. 14 we show the odd torkance of the top FM (see Eq. (3)) in the Co(3)/Cu(9)/Co(3) trilayer as a function of the lifetime broadening Γ . At large broadening of $\Gamma = 100\text{meV}$ the component $t_{xx}^{\text{top},o}$ is smaller than $t_{yy}^{\text{top},o}$ by 3%. At medium broadening of $\Gamma = 10\text{meV}$ the component $t_{xx}^{\text{top},o}$ is larger than $t_{yy}^{\text{top},o}$ by 2.7%. At small broadening of $\Gamma = 1\text{meV}$ the component $t_{xx}^{\text{top},o}$ is larger than $t_{yy}^{\text{top},o}$ by a factor of 3.5. Thus, like in the case of the even SOT, we find that the anisotropy of the torkance with respect to the in-plane rotation of the applied electric field reduces with increasing lifetime broadening Γ . However, the reduction of this anisotropy with increasing Γ is much more abrupt than in the case of the even SOT and cannot be explained by the reduction of the spin-diffusion length. We attribute the strong anisotropy of the odd SOT at

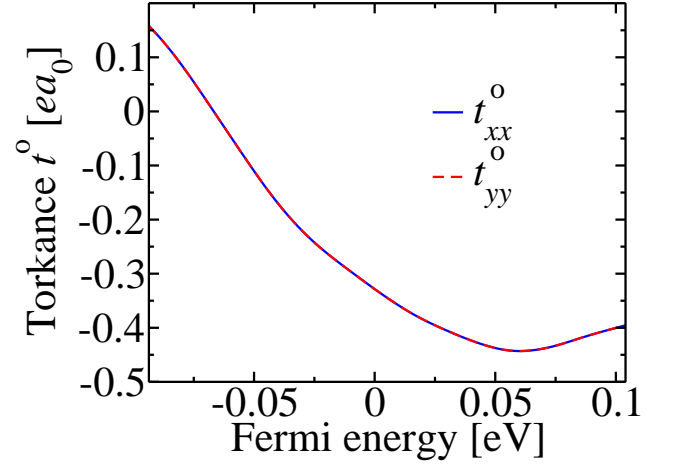


FIG. 13: Odd torkance t_{ij}^o in the Co(3)/Cu(9) bilayer vs. Fermi energy \mathcal{E}_F when $\theta = \phi = 0$ and $\Gamma = 25\text{meV}$.

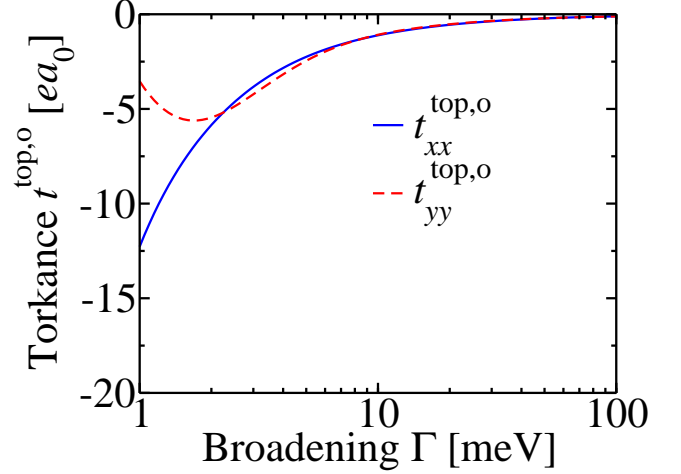


FIG. 14: Odd torkance $t_{ij}^{\text{top},o}$ on the top magnet in the Co(3)/Cu(9)/Co(3) trilayer vs. lifetime broadening Γ when $\theta = \phi = 0$.

small Γ to the anisotropy of the Fermi surface, which is induced by the bottom FM. For medium and large values of Γ the odd SOT is less sensitive to this Fermi surface anisotropy than for small Γ .

For comparison, we show in Fig. 15 the total odd torkance (see Eq. (4)) in the Co(3)/Cu(9) bilayer as a function of the lifetime broadening Γ . At large broadening $\Gamma = 100\text{meV}$ t_{xx}^o in the Co(3)/Cu(9) bilayer is larger than $t_{xx}^{\text{top},o}$ in the Co(3)/Cu(9)/Co(3) trilayer by 1.7% while at small broadening $\Gamma = 1\text{meV}$ $t_{xx}^{\text{top},o}$ in the Co(3)/Cu(9)/Co(3) trilayer is larger than t_{xx}^o in the Co(3)/Cu(9) bilayer by 24%. In contrast, $t_{yy}^{\text{top},o}$ in the Co(3)/Cu(9)/Co(3) trilayer is larger than t_{yy}^o in the Co(3)/Cu(9) bilayer by 1.5% at large broadening $\Gamma = 100\text{meV}$, while at small broadening $\Gamma = 1\text{meV}$ t_{yy}^o

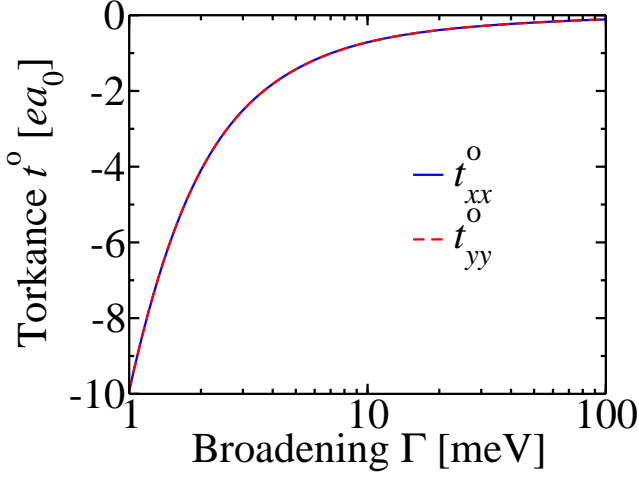


FIG. 15: Odd torkance t_{ij}^o in the Co(3)/Cu(9) bilayer vs. lifetime broadening Γ when $\theta = \phi = 0$.

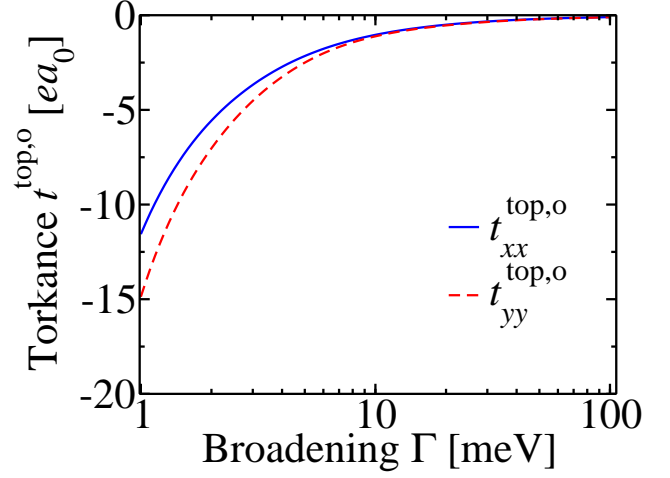


FIG. 17: Odd torkance $t_{ij}^{top,o}$ in the Co(3)/Cu(3)/Co(3) magnetic trilayer vs. lifetime broadening Γ when $\theta = \phi = 0$.

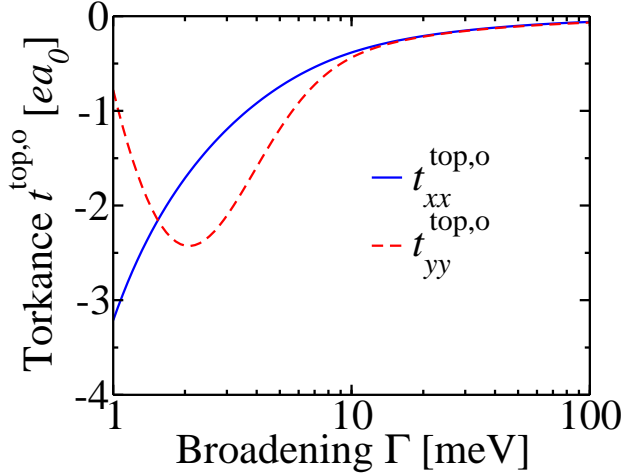


FIG. 16: Odd torkance $t_{ij}^{top,o}$ in the Co(3)/Cu(9)/Co(3) magnetic trilayer vs. lifetime broadening Γ when $\theta = \phi = 0$ and when SOI is switched off on the Cu atoms.

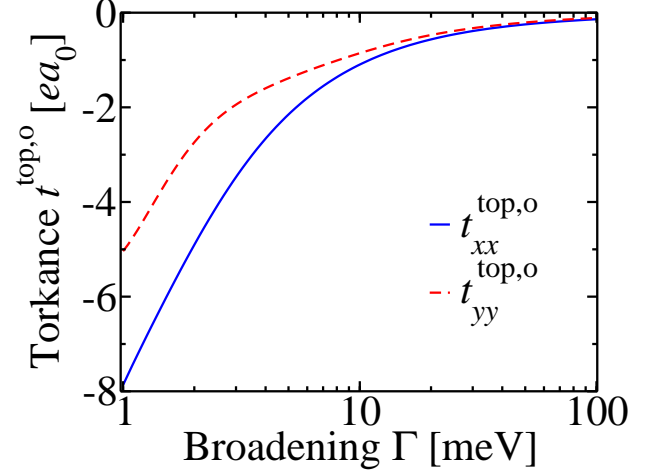


FIG. 18: Odd torkance $t_{ij}^{top,o}$ in the Co(3)/Cu(6)/Co(3) magnetic trilayer vs. lifetime broadening Γ when $\theta = \phi = 0$.

in the Co(3)/Cu(9) bilayer is larger than $t_{yy}^{top,o}$ in the Co(3)/Cu(9)/Co(3) trilayer by a factor of 2.8. Thus, the odd torques in the Co(3)/Cu(9)/Co(3) trilayer are almost identical to those in the Co(3)/Cu(9) bilayer when the broadening Γ is large, while for small broadening in particular the yy component of the torkance tensor differs significantly between the bilayer and the trilayer.

In order to discuss the contribution of SOI in Cu to the odd torque we show in Fig. 16 the torkance $t_{ij}^{top,o}$ as a function of lifetime broadening Γ when SOI is switched off on the Cu atoms. Compared to Fig. 14 the torkance is strongly decreased when SOI is switched off on the Cu atoms. This is a remarkable difference to the even torques, for which we discussed above that switching off SOI on Cu has a small influence.

In order to investigate the dependence of the odd torque on the thickness of the Cu spacer layer, we show the odd torkances of Co(3)/Cu(3)/Co(3) and Co(3)/Cu(6)/Co(3) in Fig. 17 and in Fig. 18, respectively. Like in the case of the even torkance discussed in the previous subsection, the odd torkances of Co(3)/Cu(3)/Co(3), Co(3)/Cu(6)/Co(3), and Co(3)/Cu(9)/Co(3) are similar for sufficiently large Γ and differ substantially for small Γ .

In Fig. 19 we show the odd torkance in the Co(3)/Cu(9)/Co(3) trilayer as a function of the angle θ when $\phi = 0$ and $\Gamma = 25\text{meV}$. We plot the θ and ϕ components of the torkance defined in Eq. (15) and in Eq. (16), respectively. The torkance $t_{\phi y}^{top,o}$ vanishes at $\theta = 90^\circ$ in agreement with the symmetry analysis in Table II. However, $t_{\theta x}^{top,o}$ increases strongly from $t_{\theta x}^{top,o} = -0.44ea_0$

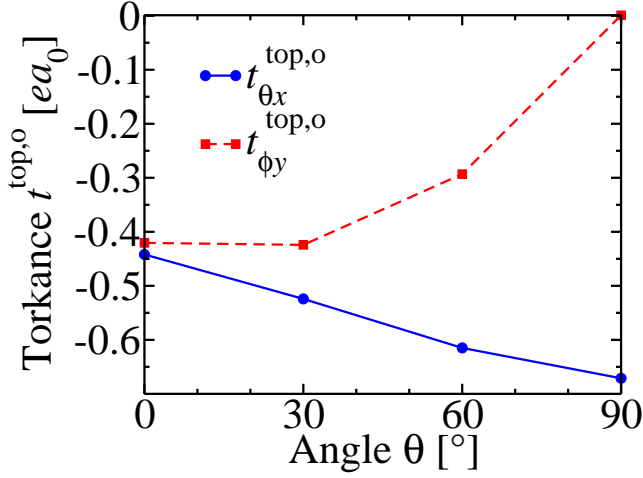


FIG. 19: Odd torkance $t_{\theta x}^{\text{top},o}$ (circles) and odd torkance $t_{\phi y}^{\text{top},o}$ (squares) in the Co(3)/Cu(9)/Co(3) magnetic trilayer vs. angle θ when $\phi = 0$ and $\Gamma = 25\text{meV}$. Lines serve as guide to the eye.

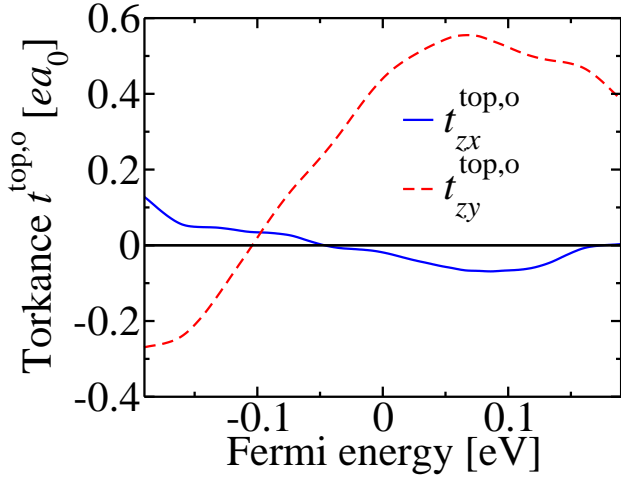


FIG. 20: Odd torkance $t_{ij}^{\text{top},o}$ in the Co(3)/Cu(9)/Co(3) magnetic trilayer vs. Fermi energy \mathcal{E}_F when $\theta = \phi = 90^\circ$ and $\Gamma = 25\text{meV}$.

($\theta = 0^\circ$) to $t_{\theta x}^{\text{top},o} = -0.67ea_0$ ($\theta = 90^\circ$). As discussed above, a similar increase occurs for the even torkance $t_{\phi x}^{\text{top},e}$ shown in Fig. 9. One contribution to the increase of $t_{\theta x}^{\text{top},o}$ with the angle θ may come from the z -polarized spin current present in trilayers, because it is expected to provide a term proportional to $\sin(\theta)$. However, experimentally a strong angular dependence of the odd torque is also found in bilayers such as $\text{AlO}_x/\text{Co}/\text{Pt}$ and $\text{MgO}/\text{CoFeB}/\text{Ta}$ [5].

In Fig. 20 we show the odd torkance as a function of Fermi energy \mathcal{E}_F when $\theta = \phi = 90^\circ$. In agreement with the symmetry analysis in Table II the odd SOT points in z direction in this case, and it can be generated by an

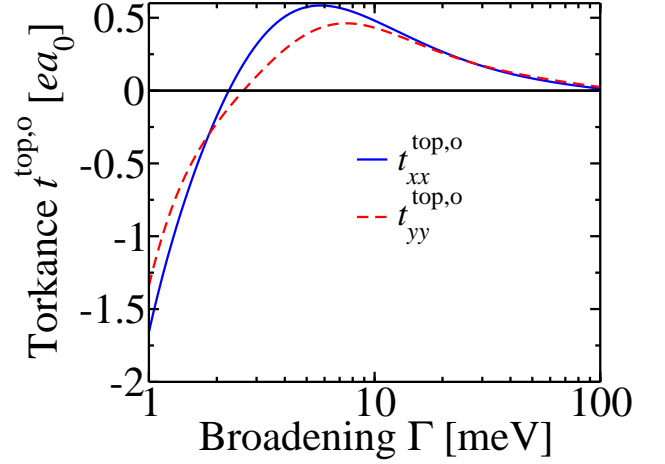


FIG. 21: Odd torkance $t_{ij}^{\text{top},o}$ in the Co(3)/Pt(13)/Co(3) magnetic trilayer vs. broadening Γ when $\theta = \phi = 0^\circ$.

electric field in x direction, but also by an electric field in y direction. As discussed at the end of Sec. II, we attribute $t_{zx}^{\text{top},o}$ to a spin current with spin-polarization along z direction flowing from the bottom Co layer to the top Co layer and assume that this spin current is generated at the bottom FM interface through spin-orbit precession. $t_{zx}^{\text{top},o}$ is small at $\mathcal{E}_F = 0$ and therefore also the z -polarized spin current is small. The z -polarized spin current therefore provides only a small contribution to the θ -dependence of $t_{\theta x}^{\text{top},o}$ shown in Fig. 19.

Finally, we discuss the odd torque in the Co(3)/Pt(13)/Co(3) trilayer. In Fig. 21 we show the odd torkance as a function of the lifetime broadening Γ when $\theta = \phi = 0^\circ$. Similar to the Co/Cu/Co trilayers, the difference between $t_{xx}^{\text{top},o}$ and $t_{yy}^{\text{top},o}$ is pronounced only at small Γ . Remarkably, for small and medium values of Γ the odd torkance in the Co(3)/Pt(13)/Co(3) trilayer is smaller than the one in the Co/Cu/Co trilayers, showing again that sizable SOTs can be observed even in trilayers that are composed only of $3d$ transition metals.

V. DMI IN Co/Cu/Co TRILAYERS

Since DMI and SOT are related in various ways [20–22], we expect the DMI in Co/Cu/Co trilayers to be anisotropic due to the bottom FM like the SOT, the anisotropy of which we discussed above. We calculate the DMI according to Eq. (10) for magnetization along z in the top magnet. In Table III we show the layer-resolved DMI coefficients for the Co/Cu/Co trilayer and for the Co/Cu bilayer. The largest contribution to the DMI arises from Co-1, which is adjacent to vacuum. The contributions from Co-3, which is adjacent to the cop-

per layer, are significantly smaller and opposite in sign. The contributions from Co-3 are small, because the SOI in Cu is small. As expected, the DMI is anisotropic in Co/Cu/Co, because the magnetization in the bottom FM points in x direction. The DMI free energy density Eq. (7) of a flat right-handed cycloidal spin spiral parallel to the xz plane with wave vector q in x direction is $D_{yx}q$ while the DMI free energy density of a flat right-handed cycloidal spin spiral parallel to the yz plane with wave vector q in y direction is $-D_{xy}q$. These two energy densities differ by 7%.

TABLE III: Layer-resolved DMI-coefficients for the Co/Cu/Co trilayer and for the Co/Cu bilayer. The sums of the contributions from layers Co-1, Co-2, Co-3 and Cu-1 are listed in the line D_{ij}^{top} (see Eq. (9)). For Co/Cu only D_{xy} is shown, because $D_{yx} = -D_{xy}$ due to symmetry in this case. $D_{yx} \neq -D_{xy}$ for Co/Cu/Co, because the bottom magnet reduces the symmetry. The DMI coefficients are specified in units of meVÅ per unit cell (uc).

	Co/Cu/Co		Co/Cu
	D_{xy} [meVÅ/uc]	D_{yx} [meVÅ/uc]	D_{xy} [meVÅ/uc]
Co-1	-3.07	2.80	-3.78
Co-2	-0.878	1.07	-0.58
Co-3	1.24	-0.94	0.48
Cu-1	-0.017	0.014	-0.01
D_{ij}^{top}	-2.73	2.94	-3.89

This anisotropy provides a simple way to tune the DMI. For a cycloidal spin spiral that propagates in a given fixed direction in the top magnet one can change the angle between the spin-spiral wave vector and the bottom FM magnetization by rotating the latter. Thereby one can tune the DMI and as a consequence the wavelength of the spin spiral. While the anisotropy of DMI is only 7% in Co/Cu/Co according to our calculations, we expect that larger anisotropies can be realized by optimizing the composition of the trilayer with the goal of maximizing this effect. In systems with anisotropic DMI skyrmions are of elliptic shape instead of circular shape. By rotating the magnetization in the bottom layer one may rotate these ellipsoids and thereby excite the skyrmions.

VI. SUMMARY

We find that SOT and DMI in Co/Cu bilayers and Co/Cu/Co trilayers are larger than what one might expect from the small SOI of Cu. A small torque per current ratio in Co/Cu bilayers is therefore the result of the high electrical conductivity of Cu and not the consequence of a small SOT torque. This is consistent with recent experiments showing SOT-switching in trilayers that contain only 3d transition-metal elements.

Co/Cu/Co can serve as a model system to study SOTs in magnetic trilayers that are composed of 3d transition metals only. The SOT is anisotropic in Co/Cu/Co when the magnetization of the bottom magnet is in-plane and the magnetization of the top magnet is out-of-plane, i.e., the SOT depends on the in-plane direction of the applied electric current. We find the anisotropy of the even torque to be particularly large and attribute it to spin currents that are generated at the bottom magnet. The even torque is significantly enhanced when the applied electric field is aligned with the in-plane magnetization of the bottom magnet. In contrast, when the electric field is applied perpendicularly to the in-plane magnetization of the bottom layer, the even torque in Co/Cu/Co trilayers is found to be similar to the even torque in Co/Cu bilayers. When the magnetizations of both the bottom and the top magnet are in-plane, but perpendicular to each other, we observe a nonlocal SOT that is mediated by a spin current with spin polarization along the out-of-plane direction. Additionally, we find that DMI is anisotropic in Co/Cu/Co trilayers, i.e., we predict that the width of domain walls and the spin-spiral wave number of spin-spirals depend on their in-plane orientation. Therefore, we expect that the rotation of the magnetization direction of the bottom magnet in magnetic trilayers similar to Co/Cu/Co provides an easy way to tune the DMI.

Acknowledgments

We gratefully acknowledge computing time on the supercomputers of Jülich Supercomputing Center and RWTH Aachen University as well as funding by Deutsche Forschungsgemeinschaft (MO 1731/5-1).

* Corresp. author: f.freimuth@fz-juelich.de

- [1] A. Manchon, I. M. Miron, T. Jungwirth, J. Sinova, J. Zelezny, A. Thiaville, K. Garello, and P. Gambardella, ArXiv e-prints (2018), 1801.09636.
- [2] L. Liu, C.-F. Pai, Y. Li, H. W. Tseng, D. C. Ralph, and R. A. Buhrman, *SCIENCE* **336**, 555 (2012).
- [3] C.-F. Pai, L. Liu, Y. Li, H. W. Tseng, D. C. Ralph, and R. A. Buhrman, *Appl. Phys. Lett.* **101**, 122404 (2012).
- [4] F. Freimuth, S. Blügel, and Y. Mokrousov, *Phys. Rev. B* **90**, 174423 (2014).
- [5] K. Garello, I. M. Miron, C. O. Avci, F. Freimuth, Y. Mokrousov, S. Blügel, S. Auffret, O. Boulle, G. Gaudin, and P. Gambardella, *Nature Nanotech.* **8**, 587 (2013).
- [6] W. Zhang, M. B. Jungfleisch, W. Jiang, J. E. Pearson, A. Hoffmann, F. Freimuth, and Y. Mokrousov, *Phys. Rev. Lett.* **113**, 196602 (2014).
- [7] S. Fukami, C. Zhang, S. DuttaGupta, A. Kurenkov, and H. Ohno, *NATURE MATERIALS* **15**, 535 (2016).
- [8] H. Reichlová, D. Krieger, V. Holý, K. Olejník, V. Novák, M. Yamada, K. Miura, S. Ogawa, H. Taka-

- hashi, T. Jungwirth, et al., Phys. Rev. B **92**, 165424 (2015).
- [9] T. Taniguchi, J. Grollier, and M. D. Stiles, Phys. Rev. Applied **3**, 044001 (2015).
- [10] D. A. Pesin and A. H. MacDonald, Phys. Rev. B **86**, 014416 (2012).
- [11] X. Wang and A. Manchon, Phys. Rev. Lett. **108**, 117201 (2012).
- [12] P. M. Haney, H.-W. Lee, K.-J. Lee, A. Manchon, and M. D. Stiles, Phys. Rev. B **88**, 214417 (2013).
- [13] S.-h. C. Baek, V. P. Amin, Y.-W. Oh, G. Go, S.-J. Lee, G.-H. Lee, K.-J. Kim, M. D. Stiles, B.-G. Park, and K.-J. Lee, Nature Materials (2018), URL <https://doi.org/10.1038/s41563-018-0041-5>.
- [14] A. M. Humphries, T. Wang, E. R. J. Edwards, S. R. Allen, J. M. Shaw, H. T. Nembach, J. Q. Xiao, T. J. Silva, and X. Fan, Nature Communications **8**, 911 (2017).
- [15] V. P. Amin and M. D. Stiles, Phys. Rev. B **94**, 104419 (2016).
- [16] V. P. Amin and M. D. Stiles, Phys. Rev. B **94**, 104420 (2016).
- [17] V. P. Amin, J. Zemen, and M. D. Stiles, ArXiv e-prints (2018), 1803.00593.
- [18] F. Freimuth, S. Blügel, and Y. Mokrousov, Phys. Rev. B **92**, 064415 (2015).
- [19] L. Wang, R. J. H. Wesselink, Y. Liu, Z. Yuan, K. Xia, and P. J. Kelly, Phys. Rev. Lett. **116**, 196602 (2016).
- [20] K.-W. Kim, H.-W. Lee, K.-J. Lee, and M. D. Stiles, Phys. Rev. Lett. **111**, 216601 (2013).
- [21] A. J. Berger, E. R. J. Edwards, H. T. Nembach, J. M. Shaw, A. D. Karenowska, M. Weiler, and T. J. Silva, ArXiv e-prints (2016), 1611.05798.
- [22] F. Freimuth, S. Blügel, and Y. Mokrousov, Journal of physics: Condensed matter **26**, 104202 (2014).
- [23] R. V. Mikhaylovskiy, E. Hendry, A. Secchi, J. H. Mentink, M. Eckstein, A. Wu, R. V. Pisarev, V. V. Kruglyak, M. I. Katsnelson, T. Rasing, et al., Nature Communications **6**, 8190 (2015).
- [24] F. Freimuth, S. Blügel, and Y. Mokrousov, Phys. Rev. B **96**, 054403 (2017).
- [25] J. A. Katine, F. J. Albert, R. A. Buhrman, E. B. Myers, and D. C. Ralph, Phys. Rev. Lett. **84**, 3149 (2000).
- [26] P. M. Haney, D. Waldron, R. A. Duine, A. S. Nunez, H. Guo, and A. H. MacDonald, Phys. Rev. B **76**, 024404 (2007).
- [27] C. Heiliger, M. Czerner, B. Y. Yavorsky, I. Mertig, and M. D. Stiles, J. Appl. Phys. **103**, 07A709 (2008).
- [28] G. Géranton, B. Zimmermann, N. H. Long, P. Mavropoulos, S. Blügel, F. Freimuth, and Y. Mokrousov, Phys. Rev. B **93**, 224420 (2016).
- [29] F. Freimuth, R. Bamler, Y. Mokrousov, and A. Rosch, Phys. Rev. B **88**, 214409 (2013).
- [30] F. Freimuth, S. Blügel, and Y. Mokrousov, J. Phys.: Condens. matter **28**, 316001 (2016).
- [31] See <http://www.flapw.de>.
- [32] J. P. Perdew, K. Burke, and M. Ernzerhof, Phys. Rev. Lett. **77**, 3865 (1996).
- [33] H. Krakauer, M. Posternak, and A. J. Freeman, Phys. Rev. B **19**, 1706 (1979).
- [34] P. Kurz, F. Förster, L. Nordström, G. Bihlmayer, and S. Blügel, Phys. Rev. B **69**, 024415 (2004).
- [35] N. Marzari, A. A. Mostofi, J. R. Yates, I. Souza, and D. Vanderbilt, Rev. Mod. Phys. **84**, 1419 (2012).
- [36] F. Freimuth, Y. Mokrousov, D. Wortmann, S. Heinze, and S. Blügel, Phys. Rev. B **78**, 035120 (2008).
- [37] A. A. Mostofi, J. R. Yates, Y.-S. Lee, I. Souza, D. Vanderbilt, and N. Marzari, Computer Physics Communications **178**, 685 (2008).
- [38] Y. Yao, L. Kleinman, A. H. MacDonald, J. Sinova, T. Jungwirth, D.-s. Wang, E. Wang, and Q. Niu, Phys. Rev. Lett. **92**, 037204 (2004).
- [39] K. M. Seemann, Y. Mokrousov, A. Aziz, J. Miguel, F. Kronast, W. Kuch, M. G. Blamire, A. T. Hindmarch, B. J. Hickey, I. Souza, et al., Phys. Rev. Lett. **104**, 076402 (2010).
- [40] J. Kübler and C. Felser, Phys. Rev. B **85**, 012405 (2012).
- [41] H. X. Yang, M. Chshiev, B. Dieny, J. H. Lee, A. Manchon, and K. H. Shin, Phys. Rev. B **84**, 054401 (2011).
- [42] A. R. Mellnik, J. S. Lee, A. Richardella, J. L. Grab, P. J. Mintun, M. H. Fischer, A. Vaezi, A. Manchon, E. A. Kim, N. Samarth, et al., NATURE **511**, 449 (2014).